Contract Number ICA4-CT-2002-10012

Efficient Operation of Urban Wastewater Treatment Plants

Diagnosis algorithms for robustly detecting and isolating of a number of sensor, actuator or/and process faults for discontinues SBR Deliverable D6.1

Deliverable type: Report

Number: D6.1

Date of delivery: 1st September 2005

Task: WP6 - Fault Detection and Isolation

Responsible:

C. Verde

Instituto de Ingeniería, UNAM

México

E-mail: cverde@servidor.unam.mx

Other Contributors:

D. Wimberger

J. Mina

J. Cuellar

Instituto de Ingeniería, UNAM

México

Contents

1 Introduction

This document presents the diagnosis algorithms developed for the fault detection and isolation (FDI) of the selected devices and components of the process. The goal of each algorithm is to provide on-line information about structure changes and parameters deviations of components and devises of the process from the nominal situation. The analysis and discussion of the critical fault and cases to be considered in EOLI were given in D1.4 and the selected cases are specifically:

- Membrane damage of a dissolved oxygen sensor of type Clark.
- Damages in the Servo-Valve with three cases; valve clogging, plug or seat sedimentation and plug or seat erosion.
- Fault conditions in the model EM1 characterized by strong deviations of the inhibition parameter K_i and the affinity constant K_s of the Haldane or Andrews kinetics model.

This deliverable reports the algorithm developed for each of the three components.

2 Distributed FDI Scheme

Taking into account the goal of the EOLI project (design of a low cost, modular and reliability system) and the low capacity of the measurements of the SBR to capture its internal variables for all possible conditions, (Figueroa, 2002), (Vargas, 2003), we tackled the fault diagnosis for actuators and sensors separately from those of the process using a distributed FDI scheme. Thus, the specific diagnosis algorithms for faults in the dissolved oxygen (DOx) sensor and servo-valve actuator are considered separately and the detection of specific abnormal symptoms in the reactor can be implemented alone and independent on each installation.

Considering that the shut-down time in the reactor is mainly due to the lack of confidence in the information provided by the instrumentation and faulty actuators, a modular and distributed fault detection and isolation system can have more potential benefit that a fault diagnosis system in a overall unit scheme. Therefore, the fault detection and isolation tasks in the EOLI project are designed using the distributed structure

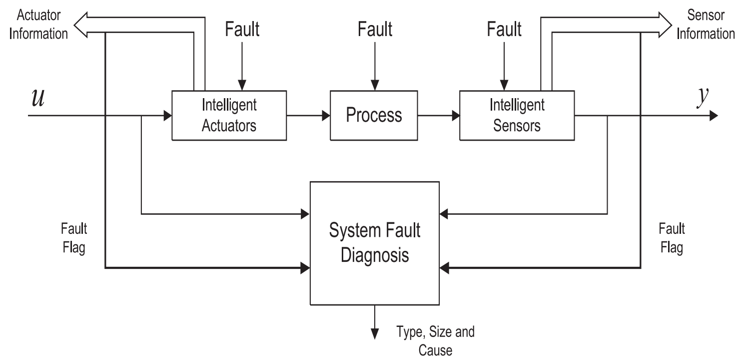

Figure 1: Faul Detection Scheme

shown in Fig. 2 in which the sensors and actuators fault diagnosis are separated from the process at the first level. This fault detection scheme despairs the machine intelligence away from centralized computer towards distributed fieldbus devices and allows to capture in an abstract structure the monitoring functions, as they are implemented in most practical cases. It is to remark that a distributed fault diagnosis system must integrate the partial information given by sensors and actuators with the abnormal condition of the process in order to fire the alarm signals using the human-machine interface.

It is to note that the computational capabilities of the new hardware allows to implement this distributed scheme designing smart instruments with autonomous diagnosis tasks and minimal information of the process under supervision. Fig.2 shows the communication between the smart sensors and actuators in a distributed FDI system.

An advantage of this scheme is its modularity, since new fault cases or new sensors and actuators can be integrated in the future without requiring redesign of the system, i.e. each indicator of a fault works independently of the others at the basic level and therefore reliability of the system can be improved. Then sensors and actuators must include specific fault tests for each device but the same detection algorithm can be used without regard to the process. So the FDI system for each sensor and actuator demands an extra effort in the design, but this is compensated with the benefit related with modularity, transportability and information interchange with other levels in the supervision structure.

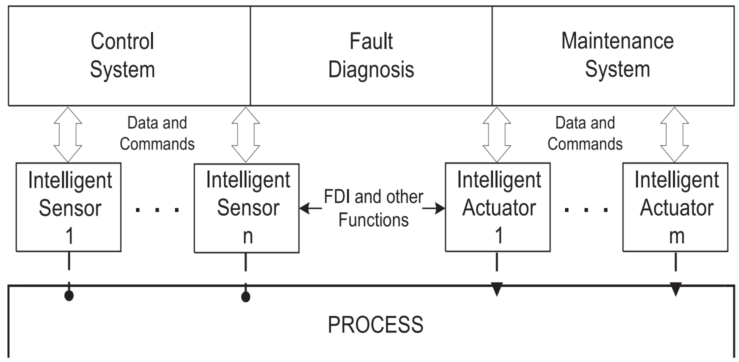

Figure 2: Communication of a distributed FDI system

3 Self Diagnosis of a Dissolved Oxygen Sensor

In the SBR process, the dissolved oxygen sensor is a key instrument during the reaction phase, since the variation of the DOx concentration in the bulk liquid in related with the oxygen transfer of the reactor and the respiration rate of the microorganisms. Moreover, since the dissolved oxygen is the only measurable state variable in the models developed by WP2, the process information could be mainly recovered by software only from the DOx sensor. Therefore, taking into account the cycles of the SBR, EOLI team developed a diagnosis algorithm which can be periodically used when the process is not in the reaction phase and it is based on the transient response of a internal current of the sensor. It is to note that the test requires to integrate specific hardware component for a real implementation.

The algorithm is designed considers the most common DOx sensor called of Clark cell which is based on an electrochemical cell for generating an electric current by chemical means. The cell has three basic components the electrolyte, the cathode and the anode. A Teflon membrane acts as a semi-permeable barrier which allows oxygen molecules to diffuse from the fluid into the sensor. A characteristic of this sensor is its low dynamic response which is dominated by the membrane diffusion process, approximately 2 min in clean condition. This diffusion process is affected if small particles are adhered to the membrane or it is damaged.

There are several possible faults associated with a DOx sensor like fouling, membrane rupture and electrolyte depletion. Attention was focused on fouling and damage in the

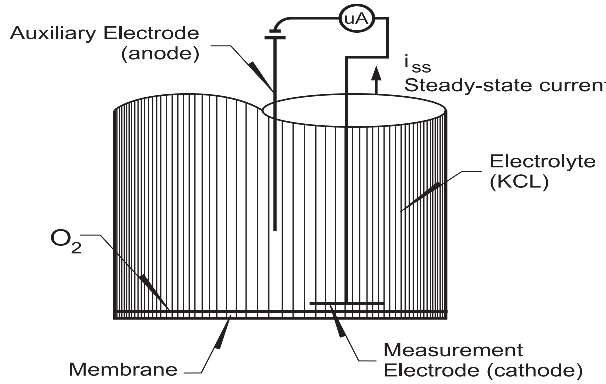

Figure 3: Schematic diagram of the DOx sensor probe

membrane.

3.1 Methodology

The transducer behavior can be explained using the simplified diagram of the Fig. 3 where the path for the oxygen molecules passing through to the electrolyte is the membrane. When a voltage B is applied between cathode and anode, the oxygen molecules in the electrolyte around the electrode begin to be consumed causing a high initial current and eventually the DOx level inside of the electrolyte reaches an equilibrium generating a steady state current in the circuit. Hence, the magnitude of the steady state current is dependent on the dissolved oxygen level in the process.

In particular, the steady state current is given by (Clarke and Fraher, 1996)

$$iss = \frac{4AFD_m H_m p_w}{b}(O_2)_w \tag{1}$$

where the subscripts m and w refer to the membrane and external fluid respectively, A is the area of the electrode, D_m is the diffusivity if the membranes, F the Faradays constant, H the Henry Law coefficient for the membrane material, p_w the partial pressure and b the thickness of the membrane. This equation shows that the current in the circuit is linearly related to the DOx in the fluid $(O_2)_w$ and the proportional constant depends on D_m and thickness b.

Since the effect of a fouling level (changes in b) and a reduction in the DOx is similar in the steady state current eq. (1), one can not detect substance layers stickled in the membrane using any steady state relation in the sensor. So a transient current must be artificial generated in the circuit to identify a changes in the parameter b. This requires the existence of a time interval for the test in which the measurement is not available and the exogenous voltage must be changed to get a transient.

Because in the case of the SBR of EOLI during the settling time, the measurements of the DOx are useless, EOLI team proposes an algorithm to estimate automatically the parameter b during this phases of a cycle.
Using the Fick's second law of diffusion

$$\frac{\partial p}{\partial t} = D_m \frac{\partial^2 p}{\partial y^2} \tag{2}$$

with the boundary conditions $p(0,t) = 0$, and $p(b,t) = p_w$, after some manipulation one gets the equation of the transient response of the current in the circuit

$$i(t) = \frac{4AFH_m D_m}{bH_w}(O_2)_w \left(1 + 2\sum_{n=1}^{\infty} \exp(-\frac{(n\pi)^2 D_m t}{b^2})\right) \tag{3}$$

when the energy supply changes at time $t = 0$ from 0 to its nominal value B, holding the membrane in a fluid with a constant DOx given by $(O_2)_w$. Considering the diffusion transfer time of the sensor $\tau = \frac{b^2}{D_m}$, eq. (3) is reduced to

$$i(t) = i_{ss}\left(1 + 2\sum_{n=1}^{\infty} \exp(-\frac{(n\pi)^2 t}{\tau})\right) = i_{ss}\left(1 + g(t)\right) \tag{4}$$

with $g(t) = 2\sum_{n=1}^{\infty} \exp(-\frac{(n\pi)^2 t}{\tau})$.

Since, any changes in the thickness and diffusivity of the membrane changes the gain in steady state i_{ss} and the value of the parameter τ, two parameters must be evaluated in expression (4) to detect a damage.

Taking into account the form of the current $i(t)$, one can say that it is equivalent to the loop current of the electric circuit of Fig. 4 with a normalize impulse response $g(t)$ in the membrane. Then, one can estimate the transient response and the parameter τ, controlling the electric switch. This can be made introducing by hardware a switch between the instruments amplifier and the loop of the anode-cathode.

Since after the circuit is closed for very small time value ($t \to 0$), the exponential terms in the summation are close to one and the current value goes to infinite. Moreover, the relative sensitivity of the current with respect to τ is very small for small values of time, one suggests to transform the signal from which the estimation of τ can be obtained.

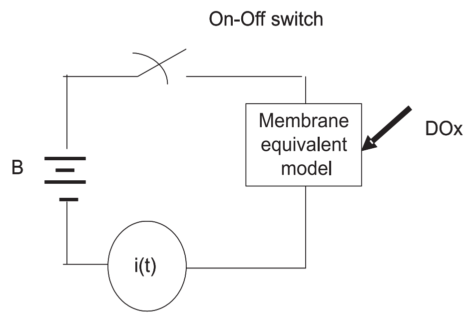

Figure 4: Equivalent Electric Circuit of the Membrane Behaviour

Then, to obtain the estimation of the parameters τ with a satisfactory precision the value of the integral of the current $i(t)$ between times $h \cong 1s$ and $2h$ has been considered as output of the system. In other words the output of the transmission during the test is given by

$$I_h = \int_h^{2h} i(t)dt = i_{ss}\left(h - \frac{2\tau}{\pi^2}\sum_{n=1}^{\infty}\frac{1}{n^2}\left\{\exp(-\frac{2(n\pi)^2 h}{\tau}) - \exp(-\frac{(n\pi)^2 h}{\tau})\right\}\right) \tag{5}$$

The rapid convergence of the terms in the summation of (5) allows to evaluate the parameter τ in a recursive way using few terms ($n = 6$) for a given I_h assuming that i_{ss} is constant during the test time interval.

Since, eq. (5) is obtained assuming zero initial condition in the membrane, a set of synchronized events must be generated in the circuit to be sure that this condition satisfies when the integral is evaluated.

Fig. 5 shows the control signals to achieve a suitable transient current in the sensor. The test of the membrane condition starts with the hold pulse which triggers a circuit to store the steady state value of the i_{ss} before the circuit is open. The three plot corresponds to the output of the hold circuit. The switch pulse defines the discharge and charge time of the membrane where the duration defines the discharge time. The last graphic corresponds to the evolution of the current in the anode-cathode circuit. The time h indicates when the integral evaluation starts.

3.2 Detector Tuning

Considering the practical values of a DOx sensor taken from (Clarke and Fraher, 1996) $b = 0.75\ \mu m$ and $Dm = 9.375\times10^{-11}\ m^2/s$, a membrane simulator has been implemented

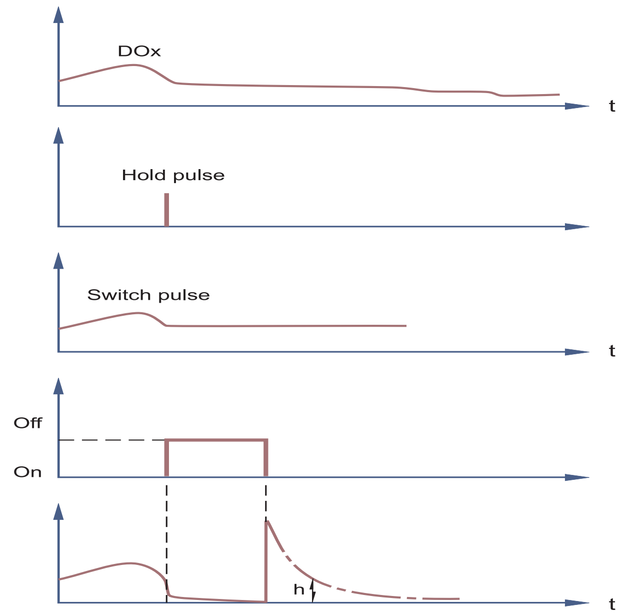

Figure 5: Control pulses and current evolution during the test interval

in Simulink software of MATLAB with the parameter $\tau = 60s$ in normal condition together with the damage detection algorithm (Cuellar, 2005). Fig. 6 shows the integration of membrane and its fault detector.

To calibrate the time value $h = h_1$, a sensitivity test for the time interval $[1 - 12]\ s$ is carried on. Table 1 shows the estimation values and the error obtained with each value. One selected a value $h = 7\ s$ for the Matlab implementation.

To characterize the tolerance of the variation in the DO_x during the test, a sensitivity analysis was carried on. Table 2 shows the estimation error of the detection algorithm when DOx is simulated as a variable signal $\sin \omega t$ with ω between $[0.0001 - 0.05]\ rad/s$. From the values of this table one concluded that the fault detection test requires approximately 10 min in which the DO_x must be constant to have an acceptable detection error (2%). This condition can be achieved during the settling and drawing phases of the process.

Complementary to the analysis of the frequency variation in DOx, the effects in its amplitude were test. Table 3

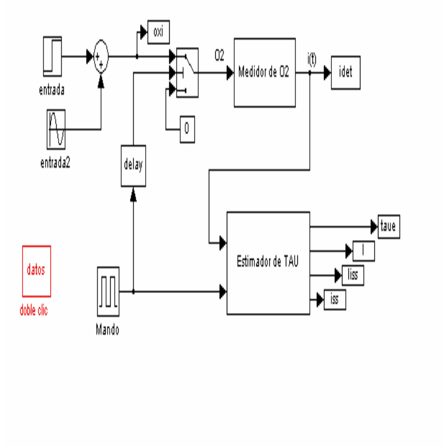

Figure 6: Implementation of the Membrane and the Damage Detection Algorithm in Simulink

Table 1: Results with a window of $h_2 = 2h_1$

h_1 [seg]	$fracIiss$	$\frac{I}{iss} - h$	τ^1 [seg]	$\%error$
1	3.6203	2.6203	59.9988	0.002
2	5.1198	3.1198	59.9981	0.0032
3	6.2706	3.2706	59.9982	0.003
4	7.2421	3.2421	59.9985	0.0025
5	8.1046	3.1046	59.9994	0.001
6	8.9001	2.9001	59.9990	0.0016
7	9.6587	2.6587	59.9997	0.0005
8	10.4019	2.4019	60.0002	0.0003
9	11.1450	2.1450	60.0005	0.0008
10	11.8980	1.8980	60.0011	0.0018
12	13.4554	1.4554	60.0024	0.004

Table 2: Results with frequency variations of the input

ω $\left[\frac{rad}{seg}\right]$	T $[seg]$	τ^1 $[seg]$	$\%error$
0.05	125.7	14.2913	76.1812
0.02	314.2	18.0807	69.8655
0.015	418.9	93.9641	56.6068
0.012	523.6	125.4178	109.0297
0.011	571.2	94.5823	57.6372
0.01	628.3	58.8287	1.9522
0.008	785.4	37.1581	38.0698
0.006	1047.2	46.5022	22.4963
0.004	1570.8	57.4996	4.1673
0.00335	1875.6	59.9821	0.0298
0.003	2094.4	61.0131	1.6885
0.001	6283.2	62.3036	3.8393
0.0009	6981.3	62.1548	3.5913
0.0005	12566.4	61.3682	2.2803
0.0001	62831.9	60.3026	0.5043

Table 3: Results with amplitude variations of the input

Amp $[V_p]$	T $[seg]$	τ^1 $[seg]$	$\%$ $error$
0.25	628.32	59.5979	0.6702
0.15	628.32	59.7843	0.3595
0.05	628.32	59.9326	0.1123

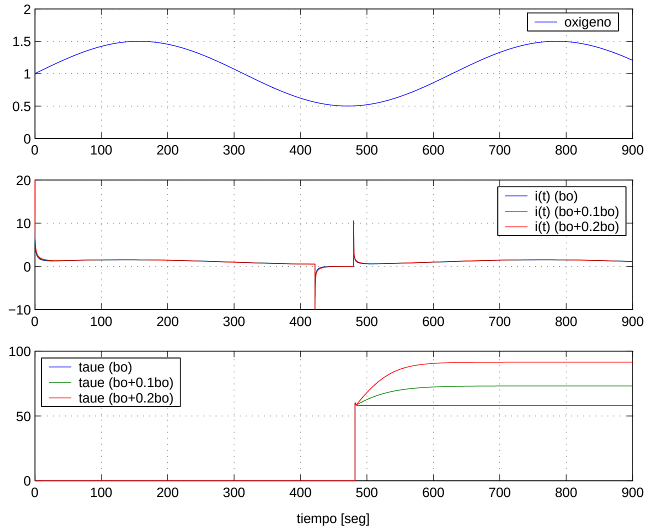

Figure 7: Results with healthy and damage membrane

3.2.1 Detector Validation

To test the methodology in the bioprocess laboratory extra sensor and hardware are required. Due to budget constraints in EOLI project, the proposed system has not been validated with the SBR process; only simulation results are feasible.

Fig. 7 shows the behavior of the estimator with clean and dirty membrane and when the electrode current is interrupted during 60 s starting at 420 s. In normal conditions the estimation yields the nominal transfer time, 60 s, and with a dirty membrane a deviation of the values is detected. Deviations of 10% and 20% of the parameter b produce increments of 12 s and 30 s in the transfer time. To trigger the fault alarm, a threshold of 15% of the nominal value is suggested.

4 Self Diagnosis of Actuators and Sensors

Due to the lack of mathematical models in general for sensors and actuators, one cannot apply FDI schemes based on explicit models. Therefore, EOLI team copes with the FDI issue using classification and pattern recognition procedures. On the other hand, the Dynamic Principal Components Analysis, DPCA, had been recognized as a powerful tool for FDI issue, since it does not require precise models. The main property of a fault detection algorithm based on DPCA (Ku *et al.*, 1995) is its capacity to distinguish if an actual observation has differences with regard to the mean and standard deviation of the reference data. This approach uses an implicit model obtained from a set of descriptive data and for the diagnosis a comparison of the actual data and the nominal pattern is achieved.

However, since DPCA assume stationary time series, if this property does not hold, high rate of false alarms are generated.

To overcome this problem EOLI team suggest to estimate on-line the means of the signals. In the following paragraph the extension of the DPCA is described and tested with a flow control servo-valve.

4.1 Dynamic Principal Component Analysis with Statistical Parameters Estimation

The objective of the novel DPCA is to keep for any normal condition the property of zero mean and unit variance by a standardization of actual data with respect to the statistical parameters estimation.

Let $\mathbf{X}$ be a set of historical data composed of n_t observations from p variables of a process, in which some of the p time series are inputs and the rest outputs, described by the matrix

$$\mathbf{X} = \begin{bmatrix} X_1 & X_2 & \cdots & X_p \end{bmatrix}_{(n_t \times p)} \tag{6}$$

To take into account the series correlation of the data, the *trajectory matrix* for each X_i

$$\mathbf{X}_i^w = \begin{bmatrix} X_i(1) & X_i(2) & \cdots & X_i(w) \\ X_i(2) & X_i(3) & \cdots & X_i(w+1) \\ \vdots & \vdots & \ddots & \vdots \\ X_i(n_t - w + 1) & X_i(n_t - w + 2) & \cdots & X_i(n_t) \end{bmatrix}_{(n \times w)}$$

$$\mathbf{X}^w = \begin{bmatrix} \mathbf{X}_1^w & \mathbf{X}_2^w & \cdots & \mathbf{X}_p^w \end{bmatrix}_{(n \times m)} \tag{7}$$

is generated, applying a 'time lag shift' of magnitude w on each one of the p columns of $\mathbf{X}$, where $n = n_t - w + 1$, $m = pw$ and w is selected considering the number of correlated lags of a signal (Elsner and Tsonis, 1996), $w = \frac{n_t}{4}$.

Assuming time invariant historical data, the mean and standard deviation vectors of $\mathbf{X}^w$ can be organized as

$$\underline{\mu} = \left[\begin{array}{cccc} \mu_1(.) & \mu_2(.) & \cdots & \mu_m(.) \end{array} \right]_{(1\times m)} \tag{8}$$

$$\underline{\sigma} = \left[\begin{array}{cccc} \sigma_1(.) & \sigma_2(.) & \cdots & \sigma_m(.) \end{array} \right]_{(1\times m)} \tag{9}$$

It is important to remark that parameters $\underline{\mu}$ and $\underline{\sigma}$ are obtained with data around a system operation point and then changes in the nominal values require re-estimations of $\underline{\widehat{\mu}}$ and $\underline{\widehat{\sigma}}$, even when the process is healthy. If exist linear relations between input and output, this re-estimation can be achieved predicting on-line components of the data matrix assuming healthy conditions.

The application of the following procedure allows to get on-line the vectors for $\underline{\widehat{\mu}}$ and $\underline{\widehat{\sigma}}$ which must be used in the DPCA for FDI instead of eqs. (8) and (9) for the case of time variant data.

4.1.1 Statistical Parameters Estimation

Consider for simplicity in the presentation a SISO system with available data x_1 and x_2 from the input and output time series, respectively

$$\mathbf{x} = \left[\begin{array}{cc} x_1 & x_2 \end{array} \right] \tag{10}$$

and assume a known linear relation between both data given by

$$x_2 = L(x_1) \tag{11}$$

Since x_1 is associated to the input data, for the statistical parameters estimation ($\underline{\widehat{\mu}}$, $\underline{\widehat{\sigma}}$) it is necessary to carry out a recursive estimation of a number of data associated with x_2.

Using the actual data $x_{1a}(k)...x_{1a}(k+w-1)$ as inputs in the relation (11), the w-output components $\widehat{x}_2(k)...\widehat{x}_2(k+w-1)$ are estimated and the row vector

$$\widehat{\mathbf{x}}^w = \left[\begin{array}{cccccc} x_{1a}(k) & \cdots & x_{1a}(k+w-1) & \widehat{x}_2(k) & \cdots & \widehat{x}_2(k+w-1) \end{array} \right]_{(1\times m)} \tag{12}$$

can be organized, and applying a single moving average (SMA) on $\widehat{\mathbf{x}}^w$, the estimated means vector is obtained

$$\underline{\widehat{\mu}} = \left[\begin{array}{cccc} \widehat{\mu}_1 & \widehat{\mu}_2 & \cdots & \widehat{\mu}_m \end{array} \right]_{(1\times m)} \tag{13}$$

$$\underline{\widehat{\sigma}} = \left[\begin{array}{cccc} \widehat{\sigma}_1 & \widehat{\sigma}_2 & \cdots & \widehat{\sigma}_m \end{array} \right]_{(1\times m)} \tag{14}$$

4.1.2 Algorithm for the Pattern Reference

1. Consider the nominal historical data matrix (7) with its statistical parameters pair given by (8) and (9), assuming stationarity in the set of historical data

2. Standardize the m columns of $\mathbf{X}^w$, with respect to (8) and (9), using the relation

$$\mathbf{x}s_{ij}^w = \frac{\mathbf{x}_{ij}^w - \mu_j}{\sigma_j} \tag{15}$$

   for $i = 1, \ldots, n$ and $j = 1, \ldots, m$. The standardized matrix $\mathbf{X}s^w$ will have zero mean and unit variance.

3. Calculate the data correlation matrix $\mathbf{R}$ from $\mathbf{X}^w$.

4. Evaluate the m eigenvalues of $\mathbf{R}$ and their unitary eigenvectors.

5. Organize the eigenvalues in decreasing order: λ_1, λ_2, ..., λ_m.

6. Define the m eigenvectors as a base for the space $\Re^m$, and construct a transformation matrix of $m \times l$ (l-principal factors), $\mathbf{V}_t = [V_1\, V_2\, ...\, V_l]$ for the reduced space $\Re^l$, where $l \leq m$.

7. Obtain the statistical model or l principal components matrix $\mathbf{Y}$ using the transformation

$$\mathbf{Y} = \mathbf{X}s^w \mathbf{V}_t \tag{16}$$

8. Generate, for each one of the l-variate observations in $\mathbf{Y}$, a behavior symptom described by the univariate statistic, Hotelling parameter T_y^2, given by

$$T_y^2 = y \mathbf{S}_Y^{-1} y^T \tag{17}$$

   where $\mathbf{S}_Y$ is the covariance matrix of $\mathbf{Y}$.

9. Select the normal condition threshold from the *probability density function* of the set of parameters T_y^2. Tracy (Tracy and Young, 1992) describes a procedure to obtain this threshold named Upper Control Limit.

It is important to note that this reference pattern obtaining procedure is carried out only one time, off-line; and during the fault detection stage are used the obtained transformation matrix $\mathbf{V}_t$ and covariance matrix $\mathbf{S}_Y$.

4.1.3 On-line Algorithm for Fault Detection

Consider again the case of a SISO system, the procedure for the on-line fault detection through the proposed algorithm based in DPCA is as follows:

1. Generate, from real data of the input and output signals, the vector of actual observations with time lag shifts of order w

$$\mathbf{x}a^{w} = \begin{bmatrix} x_{1a}(k) & \cdots & x_{1a}(k+w-1) & x_{2a}(k) & \cdots & x_{2a}(k+w-1) \end{bmatrix}_{(1\times m)} \tag{18}$$

2. Standardize the m terms in $\mathbf{x}a^{w}$, with respect to the estimated parameters (13) and (14) using the relation

$$\mathbf{x}as_{j}^{w} = \frac{\mathbf{x}a_{j}^{w} - \widehat{\mu}_{j}}{\widehat{\sigma}_{j}} \tag{19}$$

   for $j = 1, \ldots, m$. $\mathbf{x}as_{j}^{w}$ will have approximately zero mean and unit variance under normal operating conditions even before level changes in the input signal.

3. Transform the vector $\mathbf{x}as_{j}^{w}$ in the principal component subspace y_a

$$y_a = \mathbf{x}as_{j}^{w}\mathbf{V}_t$$

4. Map y_a in the univariate parameter $T_{y_a}^{2}$ through

$$T_{y_a}^{2} = y_a \mathbf{S}_{Y}^{-1} y_a^{T}$$

5. If the resulting statistic deviates from the normal condition threshold a fault is present in the system.

4.2 Fault Detection for a Flow Control Valve

On the base of the maintenance manuals of servo-valves, EOLI team selected the most commons faults in a flow control servo-valve the followings: Valve Clogging, Valve Plug or Seat Sedimentation and Valve Plug or Seat Erosion. The above DPCA algorithm was used to detect the three abnormal conditions.

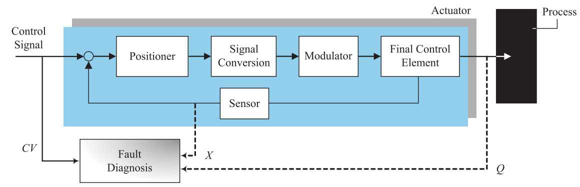

Figure 8: Actuation System with Fault Diagnosis Module

4.2.1 Scheme for Fault Diagnosis

As is depicted in Fig. 8, the fault diagnosis module is designed in such a way that it gets at every sampling period (0.5 s) the control signal CV, as input variable, and the stem displacement X, and flow Q, as output variables. On the base of these signals, one takes the advantage of the correlation between these three time series of the variables to detect and isolate some faults in the valve. To generate the time series which are associated to real data, the simulator reported in the DAMADICS (Development and Application of Methods for Actuator Diagnosis in Industrial Control Systems) benchmark (Bartys and Syfert, n.d.) is used. This benchmark consists of the valve model in Simulink, and other modules which comprise the DABLib (DAMADICS Actuator Benchmark Library).

4.2.2 Detection Results

The fault detection algorithm is adjusted considering the data matrix $\mathbf{X} = \left[\begin{array}{ccc} CV & X & Q \end{array} \right]$. Just three principal components are used for the characterization of the valve. The procedure has been evaluated considering the following cases:

(a) Normal operation of the valve with step changes in the input signal.

(b) Fault condition, *f1-Valve Clogging* of magnitude 0.75 with step changes in the input signal.

(c) Fault condition, *f2-Valve Plug or Valve Seat Sedimentation* of magnitude 0.75, with step changes in the input signal.

(d) Fault condition, *f3-Valve Plug or Valve Seat Erosion* of magnitude 0.75, with step changes in the input signal.

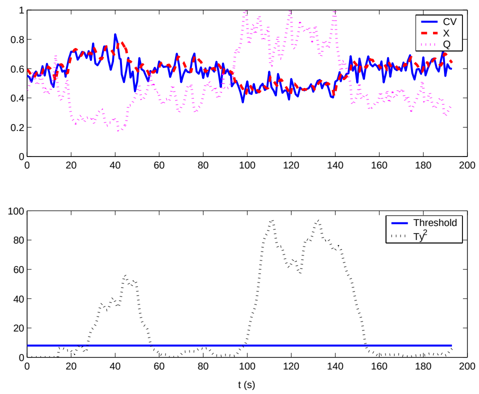

Figure 9: Step changes in CV and response of the standard DPCA based algorithm with constant means

The first evaluation has as goal to test the performance of the algorithm with respect to the step changes in the control signal CV when the valve is operating in normal conditions. One has simulated positive and negative step changes non higher than the *maximum step size* permitted for a valve ($\cong$ 10%, (InT, n.d.)) the sequence is as follows: positive step change from $(18s \leq t \leq 43s)$ and negative step change from $(93s \leq t \leq 143s)$.

As it can be seen from Fig. 9 the simple DPCA algorithm generates false alarms during the step changes in CV even when the valve is working healthy; this phenomenon is due to the absence of the stationary condition in the time series of CV, X and Q.

The response of the new algorithm with the on-line estimation of the statistical parameters is given in Fig 10 and shows the reduction of the false alarm rate. Although the stem displacement and flow estimation are not very good, this fact doesn't affect significantly the results, since the procedure requires just the output signals means.

The second part of the validation shows the response of the modified algorithm under faults $f1$, $f2$ and $f3$ of magnitude 0.75. Each fault appears at time $93s$, and the input signal is changed at $18s$ in all cases.

As it is seen in Figs. 11, 12 and 13, the values of the three behavior symptoms stay below the threshold during the step change in the input signal, and the threshold is only

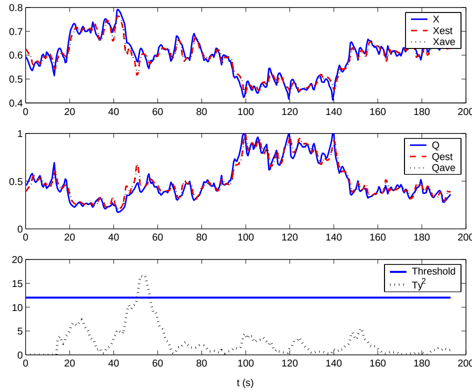

Figure 10: Actual, estimated and averaged values of variables X and Q; and response of the new algorithm in normal conditions

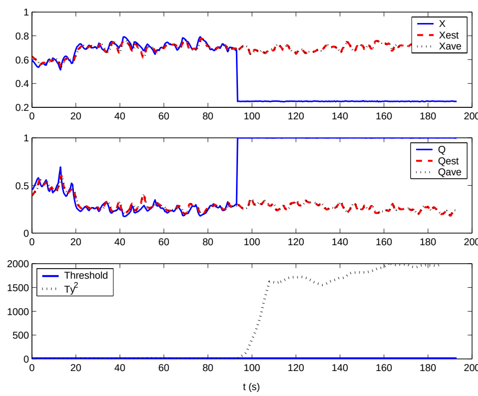

Figure 11: Detection of fault *f1-Valve Clogging* of magnitude 0.75 and with input change

exceeded when the fault is present.

The proposed modified algorithm, with on-line means estimation of the input and output signals assuming normal condition reduces the false alarms rate without demanding a precise system description. This makes this algorithm capable of deal with non stationary signals and to detect normal changes in the signals and the variations associated exclusively with the presence of fault.

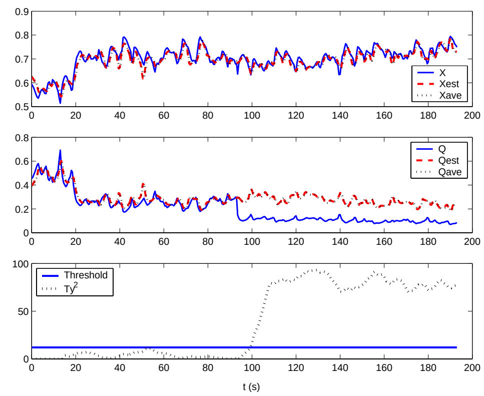

Figure 12: Detection of fault *f2-Valve Plug or Valve Seat Sedimentation* of magnitude 0.75 and with input change

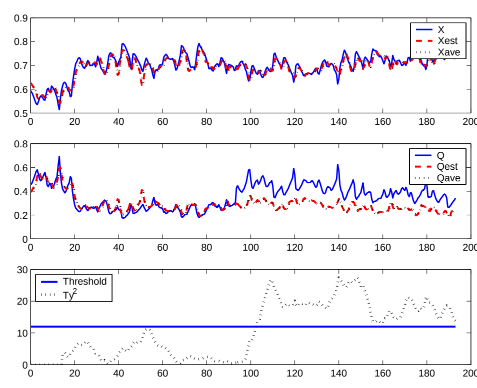

Figure 13: Detection of fault *f3-Valve Plug or Valve Seat Erosion* of magnitude 0.75 and with input change

5 FDI Algorithms for EM1 and EM2a

5.1 Estimation of Respiration Rate

The respiration rate $r(t)$ is an accepted indicator for the biomass activity and has been used for control and monitoring purposes of other bioprocesses before (Spanjers *et al.*, 1998). Although respirometric equipment is commercially available and have been used for the direct extraction of process model parameters as discussed in (Spanjers *et al.*, 1999), it represents an additional cost and maintenance factor and does not provide a continuous online estimation of *in situ* biological activities.

(Lindberg and Carlson, 1996) and (Marsili-Libelli and Vaggi, 1997) present and discuss methods for the estimation of the respiration rate in continuous WWT processes, but these cannot be applied directly to batch processes. For batch processes (Yoong *et al.*, 2000) and recently again (Puig *et al.*, 2005) describe a method for obtaining respiration rates from a batch reactor *in situ*, that is based on controlling aeration during the reaction phase to cause periods without aeration that allow to obtain the respiration rate directly from the derivative of the DO measurement. However, as a consequence it cannot provide a continuous online estimate, contrary to the method developed for the EOLI project and proposed by (Wimberger and Verde Rodarte, 2005). Nevertheless, all of these methods assume a constant volume, an assumption that does not hold during SBR operation were a change in volume will commonly occur or be desired to occur concurrently with the reaction (fed-batch mode).

5.1.1 Methodology for *In Situ* Online Estimation

The DO dynamics of an aerobic treatment process can be described using eqn. (20), a common form for chemical reactors presented by (Rawlings and Ekerdt, 2002).

$$\begin{aligned} \frac{d}{dt}\int_V O\,dV &= Q_{in}O_{in} - Q_{out}O + \\ & \int_V OTR\,dV - \int_V OUR\,dV \end{aligned} \tag{20}$$

where $OTR = K_La\,(O_{sat} - O)$, V is the reactor volume, Q_{in} the inflow rate, Q_{out} the outflow rate, O the DO concentration in the reactor, O_{in} the DO concentration in the inflow medium, K_La the oxygen mass transfer coefficient, O_{sat} the saturation DO concentration and OUR the oxygen uptake or respiration rate of the biomass, that will be denoted as r in the following.

Given a well stirred aerobic activated sludge fed batch reactor with $Q_{in} \neq 0, Q_{out} = 0$ it can be assumed that there are no concentration gradients and according to (Rawlings and Ekerdt, 2002) one can take the complete reactor volume as volume element, obtaining

$$\frac{dVO}{dt} = Q_{in}O_{in} + VK_La(O_{sat} - O) - Vr \tag{21}$$

which is equal to the first equation presented by (Spanjers *et al.*, 1999, p.119). Eq. (21) is commonly differentiated resulting

$$\frac{dO}{dt} = K_La(O_{sat} - O) - r + \frac{Q_{in}}{V}(O_{in} - O) \tag{22}$$

as proposed (Marsili-Libelli and Vaggi, 1997), where the last term $\frac{Q_{in}}{V}(O_{in} - O)$ is usually named dilution. When the volume is not assumed constant, the nonlinear dynamic equation (22) is not valid and presents difficulties which prevent a straightforward application of a linear solution for the discretization. However, an alternative new form can be obtained transforming eq. (21) into the mass balance

$$\frac{dm_o}{dt} = -r_m + Q_{in}Oin + K_La(m_{o,sat}(V) - m_o) \tag{23}$$

using the fact that $concentration = \frac{mass}{volume}$, .where m_o is the oxygen mass, $m_{o,sat}$ the oxygen mass at saturation DO concentration that now is a function of the volume and the mass respiration rate. If the dynamics of the DO sensor are comparable to the process dynamics that one wants to observe, the delay in the sensor response has to be taken into account as described by (Lindberg and Carlson, 1996).

The continuous time eq. (23) can be transformed into the discrete time eq. (24) using a Zero-Order-Hold (ZOH) as described by (Åström and Wittenmark, 1984).

$$\begin{aligned} m_o(k+1) &= k_1\, m_o(k) - k_2\, r_m(k) \\ &\quad + k_2\, K_La\, m_{o,sat} + k_2\, Q_{in}\, O_{in} \end{aligned} \tag{24}$$

where $k_1 = e^{-K_La\,h}$, $k_2 = \frac{1}{K_La}(1 - k_1)$ and h is the sampling time and k the normalized step.

The respiration rate $r_m(t)$ can be assumed to change much slower than $m_o(t)$, the corresponding model can be described by

$$r(k+t) = r(k) + n(k) \quad for\ 0 < t < 1 \tag{25}$$

where $n(k)$ is a white noise.

From eqs. (24) and (25) an observable augmented model can be obtained that is presented as

$$\begin{bmatrix} m_o(k+1) \\ r_m(k+1) \end{bmatrix} = A \begin{bmatrix} m_o(k) \\ r_m(k) \end{bmatrix} + B \begin{bmatrix} m_{o,sat}(k) \\ Q_{in}\, O_{in} \end{bmatrix} + \Gamma\, n(k) \tag{26}$$

where

$$A = \begin{bmatrix} k_1 & k_2 \\ 0 & 1 \end{bmatrix}, \ B = \begin{bmatrix} k_2\, K_L a & k_2 \\ 0 & 0 \end{bmatrix}, \ \Gamma = \begin{bmatrix} 0 \\ 1 \end{bmatrix}, C = \begin{bmatrix} 1 & 0 \end{bmatrix};$$

Eq. (26) allows observation of the mass respiration rate r_m with a full or reduced order observer. Considering the structure for the observer taken from (Åström and Wittenmark, 1984), that uses information available up to time k to provide an estimate for the respiration rate at time k, the observer for system (26) can be written as

$$\begin{aligned} \hat{m_o}(k \backslash k) \quad &= \quad (I - KC)\left(A \begin{bmatrix} m_o(k-1) \\ r_m(k-1) \end{bmatrix} + B \begin{bmatrix} m_{o,sat}(k-1) \\ Q_{in}(k-1)\, O_{in} \end{bmatrix} \right) \\ &\quad + Ky(k) \end{aligned} \tag{27}$$

where K has to be chosen such that the eq. (27) is asymptotically stable (Åström and Wittenmark, 1984). Results are obtained here using pole placement gain selection with Ackermann's formula as provided by MATLAB (Kailath, 1979) and $P = [0.2 + 0.2i\ 0.2 - 0.2i]$.

For signals with a higher noise level a useful alternative structure could be a Rauch-Tung-Striebel Fixed-Interval Optimal Smoother (discrete time) as described in (Gelb, 1974, p.164).

5.2 Process Fault Diagnosis in EM1

5.2.1 Model and Transformation

In EOLI Deliverable 2.3 (Betancur *et al.*, 2004) provided a validated model for EM1, that is based on concentrations. However, when the volume is not assumed constant, the nonlinear dynamics of the dilution term of the DO equation presents difficulties which prevent a straightforward application of a linear solution. As shown for the DO dynamics eq. (20), the complete model can be transformed into a mass balance model (conserved extensive quantities only) given by

$$\begin{aligned}
\frac{dm_x}{dt} &= \mu(V, m_s)\, m_x \qquad (28)\\
\frac{dm_s}{dt} &= -k_1\mu(V, m_s)\, m_x + q_{in}c_{s,in}\\
\frac{dm_o}{dt} &= -k_2\mu(V, m_s)\, m_x - bm_x + q_{in}c_{o,in} + K_{la}(m_{o,sat}(V) - m_o)\\
\frac{dV}{dt} &= q_{in},
\end{aligned}$$

This model is obtained using the fact that $Concentration = \frac{Mass}{Volume}$ and appreciating the fact that a measurement is available that allows to derive the actual volume in the reactor tank $V(t)$ and where $m_x, m_s, m_o, V, \mu(V, m_s), k_1, q_{in}, c_{s,in}, k_2, b, c_{o,in}, K_{la}, m_{o,sat}(v)$ are the biomass, the substrate mass, the dissolved oxygen mass, the liquid phase volume, the growth rate, the substrate to biomass conversion coefficient, the inflow rate, the concentration of substrate in the inflow , the oxygen to biomass conversion coefficient, the endogenous respiration coefficient, the dissolved oxygen concentration in the inflow, the oxygen mass transfer parameter and the dissolved oxygen mass at saturation, respectively. The growth rate as a volume dependent form can be described by

$$\mu(V) = \frac{\mu_0(V)\, m_s}{K_s(V) + m_s + \frac{m_s^2}{K_i(V)}} \qquad (29)$$

where μ_0, K_s, K_i are the specific growth rate, the half saturation coefficient and the inhibition coefficient respectively. The respiration rate is function of μ and m_x and consists of a metabolic and an endogenous part given by

$$r_m(t) = -k_2\mu(V.m_s)\, m_x - bm_x \qquad (30)$$

The parameters and coefficients identified for EM1 (Betancur *et al.*, 2004) can be used without change, assuming that $V(t)$ is available at any time through a measurement.

5.2.2 Definition of Faults

An essential part in the EM1 process model is the metabolic respiration, that is governed by the growth rate model

$$\mu = \frac{\mu_0 S}{K_s + S + \frac{S^2}{K_i}} \tag{31}$$

for inhibitory substrates (Andrews, 1968). This relation corresponds to the volume independent form of eq. (29).

Deviations in the half saturation parameter K_s and the inhibition parameter K_i have a strong and direct impact on the growth rate and as a consequence on the process dynamics. For this reason, deviations from their nominal values of $\pm\epsilon\%$ (to take into account uncertainties in the identification) are defined as process faults.

Detection and/or Diagnosis will be represented by the following sets of classes:

1. $\{$*normal, abnormal*$\}$, representing detection only
2. $\{K_i,\ K_s,\ normal\}$ representing detection and diagnosis of the parameter that changed.
3. $\{K_{i,low},\ K_{i,high},\ K_{s,low},\ K_{s,high},\ normal\}$ representing detection and diagnosis of parameter that changed as well as the direction of the change.

where *normal* stands for normal behavior, *abnormal* for a change in one of the parameters, $K_{(s,i)}$ for a change in the corresponding parameter and $K_{(s,i),(low,high)}$ for a change in the respective parameter and the direction of change.

The analytical FDI procedures for nonlinear systems based on parity relations and observers (Patton *et al.*, 2000) assume in general that the faults are additive. In the case of the EM1 model with a fault f, one gets the model description

$$\begin{aligned}
\frac{dm_x}{dt} &= \mu(V, m_s)\, m_x + \alpha_1 f \\
\frac{dm_s}{dt} &= -k_1\mu(V, m_s)\, m_x + q_{in}c_{s,in} + \alpha_2 f \\
\frac{dm_o}{dt} &= -k_2\mu(V, m_s)\, m_x - bm_x + q_{in}c_{o,in} + K_{la}(m_{o,sat}(V) - m_o) \\
\frac{dV}{dt} &= q_{in}
\end{aligned} \tag{32}$$

where constants α_i characterize the effect of the fault in the state variables.

To analyze the applicability of the analytical FDI approaches first the monitorability of the structure eq. (32) using the structural analysis, as proposed by (Blanke *et al.*, 2003) was applied. From the mass balance model (28) one can obtain the following set of constraints which is the start point of the analysis.

$$\dot{m}_x = \mu m_x \tag{c1}$$

$$\dot{m}_s = -k_1 \mu m_x + q_{in} c_{s,in} \tag{c2}$$

$$\dot{m}_o = r + K_L a(m_{o,sat} - m_o) + q_{in} c_{o,in} \tag{c3}$$

$$\dot{V} = q_{in} \tag{c4}$$

$$\mu = \frac{\mu_0 m_s}{K_s + m_s + \frac{m_s^2}{K_i}} \tag{c5}$$

$$r = -k_2 \mu m_x - b m_x \tag{c6}$$

$$m_{o,sat} = c_{o,sat} V \tag{c7}$$

$$c_{o,sat} = f(T) \tag{c8}$$

$$\dot{m}_x = \frac{dm_x}{d_t} \tag{c9}$$

$$\dot{m}_s = \frac{dm_s}{d_t} \tag{c10}$$

	q_{in}	T	c_o	V	$c_{o,in}$	m_x	m_s	m_o	μ	r	$m_{o,sat}$	$c_{o,sat}$	$\dot{m_x}$	$\dot{m_s}$	$\dot{m_o}$	$\dot{V}$	$c_{s,in}$
c_1						x			x				x				
c_2	$\acute{1}$					x			x					x			x
c_3	1				1			1		x	1				1		
c_4	1															1	
c_5							x		x								
c_6						x			x	x							
c_7				1							1	1					
c_8		1										1					
c_9						x							x				
c_{10}							x							x			
c_{11}								1							1		
c_{12}	1															1	
c_{13}			1	1				1									

Table 4: Incidence Matrix

$$\dot{m_o} = \frac{dm_o}{d_t} \tag{c11}$$

$$\dot{V} = \frac{dV}{d_t} \tag{c12}$$

$$m_o = c_o V \tag{c13}$$

Applying the matching algorithm given in (Blanke *et al.*, 2003) one obtains the Incidence Matched Matrix 4 where the first 5 columns are known variables and the rest must be calculated from the structural relations between variables; 1 indicates that the variable is known or can be evaluated from other variables and x means that the variable cannot be obtained using the known variables. Therefore the structure is not under-constrained.

From the incidence matched matrix it can be inferred that the system is not monitorable, given the fact that the variables of the constraint equations $c_1, c_2, c_5, c_9, c_{10}$ cannot be calculated from other known variables.

Based on (Bastin and Dochain, 1990) Work Package 4 of EOLI has proposed an analytical observer for the biomass and substrate with unknown μ using the transformation given by

$$z_1 = m_o + k_2 m_x \tag{33}$$

$$z_2 = m_o - \frac{k_2}{k_1} m_s \tag{34}$$

for the mass balance model equivalent. As consequence the observer can be written by (35) and (36), transformed to the mass balance model equivalent.

$$\frac{dz_1}{dt} = -b\frac{z_1 - m_o}{k_2} + K_{la}(m_{o,sat} - m_o) + q_{in}c_{o,in} \tag{35}$$

$$\frac{dz_2}{dt} = -b\frac{z_1 - m_o}{k_2} + K_{la}(m_{o,sat} - m_o) + q_{in}c_{o,in} - q_{in}c_{s,in}\frac{k_2}{k_1} \tag{36}$$

Unfortunately the resulting observer (35-36) is very sensitive with respect to the initial condition of the biomass $m_x(0)$ that is used to estimate the initial conditions $z_1(0), z_2(0)$ for the observer. It can be concluded that the analytical model of the SBR is not feasible to fault diagnostic as long as it is impossible to obtain:

1. Exact measurement of the initial biomass $m_x(0)$ with an error of maximal $\pm 5\%$.

2. Exact measurement of the substrate concentration in the inflow.

5.2.3 Methodology

An alternative to an analytical approach is a signal based approach, using feature extraction and classification for diagnosis based on historical process data. Figure 14 presents the structure of this method. The procedure consists of an offline part, which leverages historical process data and known diagnostic classifications to create a classification model using machine learning techniques. The classification model can subsequently be used online for process fault diagnosis.

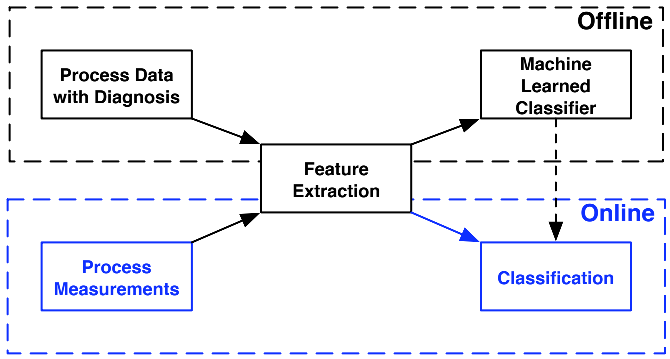

Figure 14: Diagnostic Method

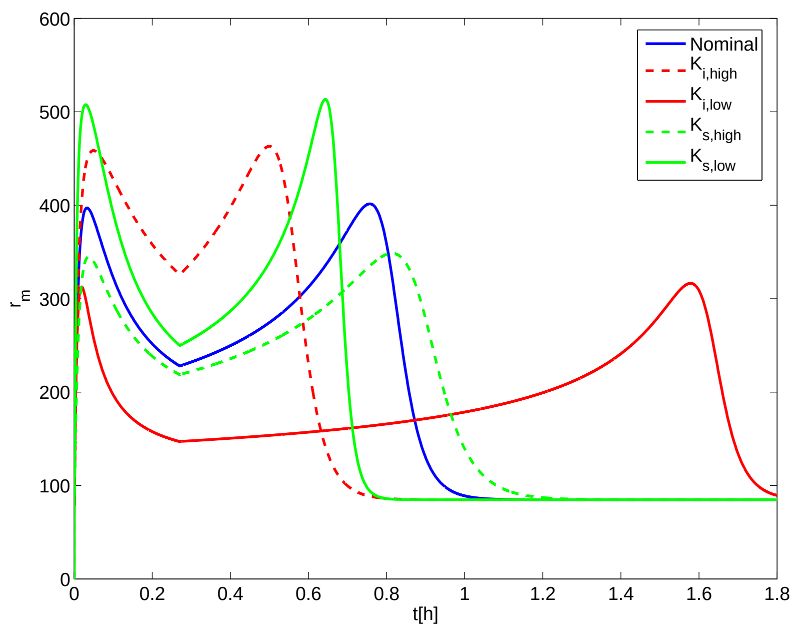

Figure 15: Respiration Profiles

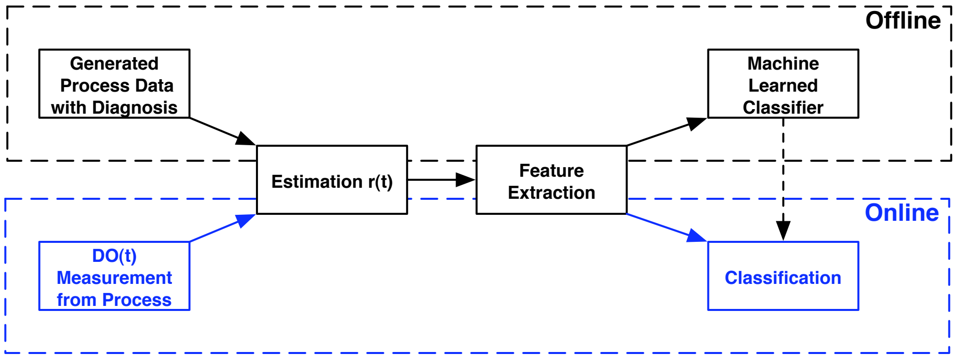

Figure 16: Diagnostic Procedure EM1

In case of the EM1 changes in the half saturation parameter K_s and the inhibition parameter K_i have a direct influence on the respiration rate profile (see Figure 15).

The formerly described methodology can be applied, in this case starting from the measurement of the dissolved oxygen, followed by the online *in situ* estimation of the respiration rate, feature extraction and classification. Due to the absence of historical process data with diagnosis, a data generator will be used for the offline part of the procedure, which is depicted in Figure 16.

The data generation will take into account the uncertainties in initial conditions and inflow concentrations, using a Monte Carlo method, that consists of taking uniform random samples from intervals [value $\pm\epsilon$%]. For each condition (constant and sampled parameters and initial values), the following sets of data are produced:

1. Changes of $\pm 50\%$ in steps of 10% in the parameters K_s and K_i (separately and not concurrently), which are tagged with the corresponding diagnostic class that indicates the type of fault.

2. To take into account uncertainties in the identification of the parameters, changes of $\pm 5\%$ in steps of 1% (separately and not concurrently), which are tagged with the diagnostic class that indicates normal behavior.

Data sets with diagnostic information are generated and accumulated for a given number (≥ 50) of randomly sampled conditions and then used for the offline part of the procedure.

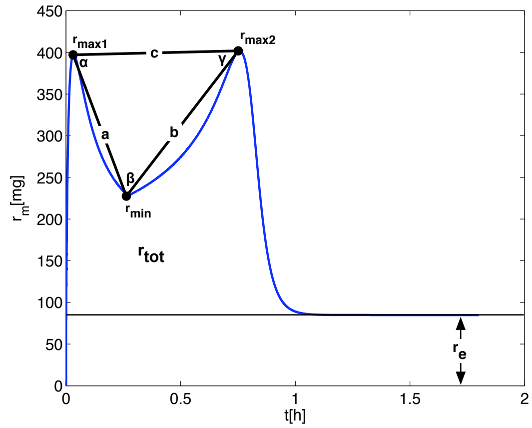

Figure 17: Nominal Respiration Rate Profile Features

5.2.4 Respiration Profile Features and Extraction

Figure 17 presents a nominal respiration rate profile obtained through simulation of EM1 with nominal conditions as presented for the validated model by (Betancur *et al.*, 2004). The proposed features that can be extracted from the curve are indicated in Figure 17.

The algorithm for the feature extraction has been implemented in MATLAB and is available in the software package that accompanies the deliverable.

5.2.5 Machine Learned Classifier and Classification

The generated feature sets tagged with corresponding diagnostic classes, are used as input for two algorithms provided by the WEKA Machine Learning Toolkit (Witten and Frank, 2000):

- J48 an implementation of the C4.5 algorithm for automatic construction of decision trees
- A Multilayer Perceptron (MLP) construction and training algorithm

Once the classifiers have been constructed from the offline simulations data, they can be used for online diagnosis.

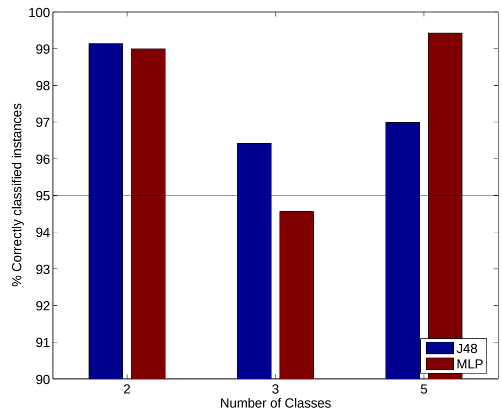

Figure 18: Results of Diagnostic Method

5.2.6 Results

The proposed method has been verified with a set of 50 simulations under following conditions:

- Uncertainties of $\pm 25\%$ in $x(0)$, the initial biomass concentration and $c_{s,in}$ the substrate concentration in the inflow are taken into account (the actual value is randomly sampled for each set of simulations)
- The inflow rate q_{in} as well as all other parameters are known and constant
- The dataset (approximately 2000 feature sets) is randomly permuted and split into training (66%) and test sets; results are presented for the test set

Results presented in Figure 18, show that the proposed method can be used to detect and diagnose the defined process faults with a relative high performance. The corresponding software package (MATLAB and Java) are available on request.

5.3 Process Fault Diagnosis in EM2a

The methodology for the extraction of the respiration rate can be applied to the case of EM2a as well. The same should be the case for the actual diagnostic procedure as described for EM1 during the aerobic phase. However, unfortunately it was not possible in the framework of EOLI given the following facts:

1. Historical process data with a clear diagnosis was not available. It means the Generated Process Data with Diagnosis of Figure 16.

2. The validated EM2a Model of EOLI reported by(Betancur *et al.*, 2004) could not reproduce the identification experiments given the same initial conditions and parameters and does not seem to capture the process dynamics with sufficient accuracy. This means that it cannot be used for the generation of the data sets with diagnosis as required by the procedure.

3. The abnormal conditions for the SBR in POLIMI reported in the deliverable D1.4 could not be generated wit the model EM2a and sufficient sets of continuous historical data are not available at this moment.

6 Conclusions

This deliverable of Work Package 6 describes the three proposed specific algorithms to tackle fault diagnosis in the SBR process in the framework of EOLI project. The fault selection was made considering the sensitivity of the process components and the available data and models to adjust and train the algorithms. Since the algorithms are generic, they can be used in any process, if the required signals are available and historical data classified in normal and abnormal conditions exits. Validation of the algorithms in real case could not be carried on, since budge limitation. However simulators of the three cases with a friendly interface are available and they could be used for operator training.

References

Andrews, J.F. (1968). A mathematical model for the continous culture of microorganisms utilizing inhibiting substrates. *Biotechnol. Bioeng.* **10**, 707–723.

Åström, K.J. and B. Wittenmark (1984). *Computer Controlled Systems*. Prentice Hall. Englewood Cliffs, UK.

Bartys, M. and M. Syfert (n.d.). *Using Damadics Actuator Benchmark Library (DABLib)*. http ://diag. mchtr.pw, edu.pl /damadics/.

Bastin, G. and D. Dochain (1990). *On-line Estimation and Adaptative Control of Bioreactors*. Elsevier Science Publishers.

Betancur, M., D. Dochain and H. Fibrianto (2004). Validated model. EOLI Deliverable 2.3. European Community Research.

Blanke, M., M. Kinnaert, J. Lunze and M. Staroswiecki (2003). *Diagnosis and Fault-Tolerant Control*. Springer Verlag. Berlin Heidelberg.

Clarke, D. W. and P. M. A. Fraher (1996). Model-based validation of a dox sensor. *Control Eng. Practice* **4**(9), 1313–1320.

Cuellar, Juventino (2005). Diagnóstico de fallas en un medidor de oxigeno disuelto. Master's thesis. Posgrado en Ingeniería, UNAM-México.

Elsner, J. B. and A. A. Tsonis (1996). *Singular Spectrum Analysis: A New Tool in Time Series Analysis*. Plenum Press, New York.

Figueroa, B. (2002). Identificabilidad teórica y práctica de los parámetros de un proceso de consumo de sustrato en un bioreactor aerobio secuencial por lotes. Master's thesis. Posgrado en Ingeniería, UNAM-México.

Gelb, Arthur, Ed.) (1974). *Applied Optimal Estimation*. The MIT Press. Cambridge, Massachusetts.

InT (n.d.). *Control Valve Dynamic Specification, Version 3.0, 11/98*.

Kailath, Thomas (1979). *Linear Systems*. Prentice Hall.

Ku, W. R., H. Storer and Ch. Georgakis (1995). Disturbance detection and isolation by dynamic principal component analysis. Technical report. Chemometrics and Intelligent Laboratory Systems, Vol. 30.

Lindberg, C.-F. and B. Carlson (1996). Estimation of the respiration rate and oxygen transfer function utilizing a slow do sensor. *Wat. Sci. Tech.* **33**(1), 325–333.

Marsili-Libelli, S. and A. Vaggi (1997). Estimation of respirometric activities in bioprocesses. *Journal of Biotechnology* **52**(3), 181–192.

Patton, R., P. Frank and R. Clark (2000). *Issues of Fault Diagnosis for Dynamic Systems.* Chap. Introduction, pp. 1–6. Springer. London.

Puig, S., L. Corominas, M. T. Vives, M. D. Balaguer and J. Colprim (2005). Development and implementation of a real-time control system for nitrogen removal using our and orp as end points. *Ind. Eng. Chem. Res.* **44**, 3367–3373.

Rawlings, J. B. and J. G. Ekerdt (2002). *Chemical Reactor Analysis and Design Fundamentals.* Nob Hill Publishing, LLC.

Spanjers, H., Imre Takács and Harry Brouwer (1999). Direct parameter extraction from respirograms for wastewater and biomass characterization. *Wat. Sci. Tech.* **39**(4), 137–145.

Spanjers, H., P.A. Vanrolleghem, G. Olsson and P.L. Dold (eds.) (1998). Respirometry in control of the activated sludge process:principles. Technical Report No.7. International Water Association.

Tracy, N. D. and J. C. Young (1992). Multivariate control charts for individual observations. *Journal of Quality Technology* **24**(2), 88–95.

Vargas, A. (2003). Observer design for nonlinear systems with reduced observability properties. PhD thesis. Posgrado en IngenierÍUNAM-México.

Wimberger, D. and C. Verde Rodarte (2005). Online monitoring of an aerobic sbr process based on dissolved oxygen measurement. In: *Proceedings of the IFAC World Congress (IFAC 2005).* p. Accepted.

Witten, I. H. and E. Frank (2000). *Practical Machine LearningTools and Techniques with Java Implementations.* Morgan Kaufmann Publishers.

Yoong, E.T., P.A. Lant and P.F. Greenfield (2000). In situ respirometry in an sbr treating waste water with high phenol concentrations. *Wat. Res.* **34**(1), 239–245.